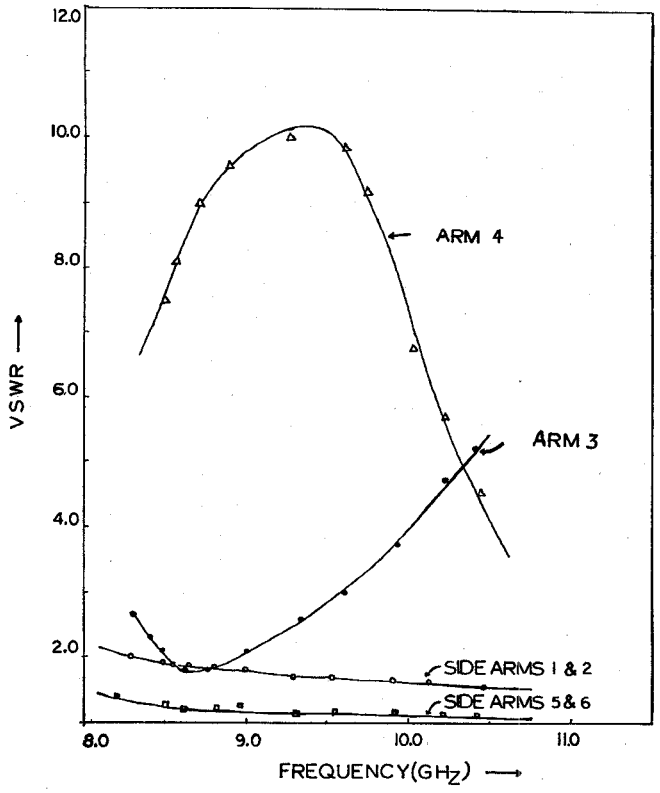

Fig. 3. The frequency response of the hybrid-T shown in Fig. 2.

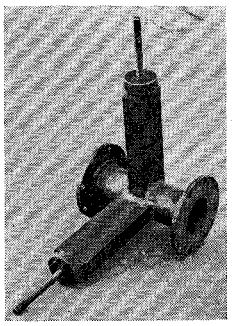

Fig. 4. A circular E–H tuner fabricated out of X-band waveguides.

insertion depth of the iris was varied to obtain a very low VSWR in this arm. The matching of port 4 was done at a frequency of 8.65 GHz where all the other ports are best matched, and a VSWR of 1.15 could be achieved in this port without affecting the VSWR in other ports by more than 5 percent.

The circular hybrid-T, using short circuits in the series and the shunt arms, is very useful where variable impedances are required to only one of the orthogonal modes propagating in the circular waveguide and in matching the circular waveguide components. By varying the position of short circuits in the series and shunt arms, a variable impedance can be offered to one of the polarizations of the collinear circular waveguide to which the series and shunt arms couple. A circular E–H tuner in the X-band and frequency range has been fabricated using the circular hybrid-T and is shown in Fig. 4. The circular E–H tuner has been successfully used to produce a VSWR of more than 100 in the frequency range 8.2–10.5 GHz. On the other hand, the circular E–H tuner has also been used to match the reflections from a circular to rectangular transition, and a VSWR of less than 1.05 could be achieved in the circular waveguide.

The circular hybrid-T discussed here could be very useful in systems applications, especially in circular waveguide networks propagating orthogonal polarized modes. As a tuner, it appears to be more useful and convenient as compared to the usual stub tuning devices.

Acknowledgment

The authors wish to thank Mr. Daljit for his help in fabrication of the device.

References

[1] C. G. Montgomery, "Techniques of microwave measurements," *Radiat. Lab. Series*, vol. 11, 1948.
[2] C. G. Montgomery, R. H. Dicke, and E. M. Purcell, "Principles of microwave circuits," *Radiat. Lab. Series*, vol. 8, 1948.

Characteristics of a Microstrip Two-Meander Ferrite Phase Shifter

WALDO M. LIBBEY

***Abstract*—A derivation for the image impedance of a microstrip line with one basic meander is presented. This shows a bandpass characteristic. A new simple technique is followed in designing a two-meander line on a G500 ferrite substrate. Scattering measurements (S band) made on a model show excellent agreement with theory. Measured nonreciprocal differential phase shift is shown.**

Introduction

In order to demonstrate that a microwave nonreciprocal network can still be practical while dependent on only a few degrees of nonreciprocal phase delay, a microstrip application is found for a ferrite phase shifter which exhibits limited but switchable differential phase.

Small amounts of nonreciprocal differential phase-shift require meander lines with only very few coupled meanders. Many formulations for conducting coupled strips in stripline assembly are given by Jones and Bolljahn [1]. One of these [1, Fig. 2(b), case 7], classified as an all-pass filter, is for a basic single meander-line configuration.

This short paper reanalyzes the basic single meander line in microstrip, taking proper account of unequal velocities for even and odd modes. The result, a modification of the Jones and Bolljahn result, shows a bandpass characteristic with a definite cutoff frequency. Further, using recent data on even- and odd-mode impedances and velocities on coupled microstrips, a matched line with two meanders is designed. Performance of an experimental model is given by scattering parameters measured at S band. Also shown are the measured nonreciprocal differential phase shift and insertion phase of this limited-meander meander line.

Theoretical Considerations

Fig. 1 shows two parallel conducting strips coupled in the microstrip transmission system which is to be considered lossless. Terminal input currents defined as in [1] and the indicated generator source currents are related by

$$i_1 = \tfrac{1}{2}(I_1 + I_2) \qquad i_3 = \tfrac{1}{2}(I_3 + I_4)$$
$$i_2 = \tfrac{1}{2}(I_1 - I_2) \qquad i_4 = \tfrac{1}{2}(I_4 - I_3). \tag{1}$$

Since infinite impedance current generators are employed, the strip voltage v_{a1} to the ground plane due to source current i_1 may be obtained from transmission-line theory as

$$v_{a1} = -j \frac{Z_{0e} i_1}{\sin \beta_e l} \cos \beta_e (l - x) \tag{2}$$

where Z_{0e} is the even-mode characteristic impedance, and $\beta_e = 2\pi f / v_e$ is the even-mode propagation constant along the strip. Similar expressions exist for contributions to v_a and v_b by the remaining current sources i_2, i_3, and i_4. For example

$$v_{a4} = -j \frac{Z_{0o} i_4}{\sin \beta_o l} \cos \beta_o x \tag{3}$$

where Z_{0o} is the odd-mode characteristic impedance, and $\beta_o = 2\pi f / v_0$ is the odd-mode propagation constant along the strip.

Manuscript received April 3, 1972; revised February 20, 1973. The initial phase of this project was contained in a Ph.D. dissertation submitted to the Department of Electrical Engineering, Worcester Polytechnic Institute, Worcester, Mass.
The author is with the Department of Electrical Engineering, University of Maine, Barrows Hall, Orono, Me. 04473.

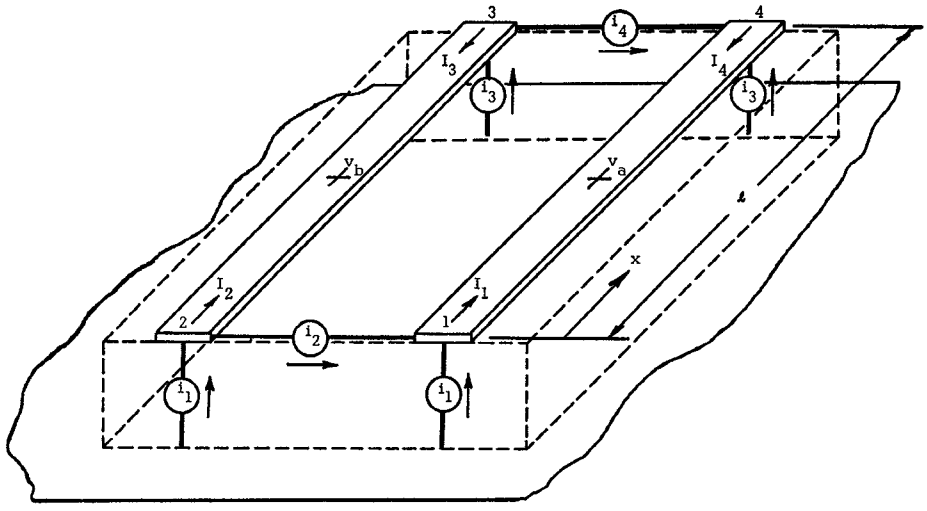

Fig. 1. Notation used in deriving the image impedance characteristic for the microstrip basic meander line.

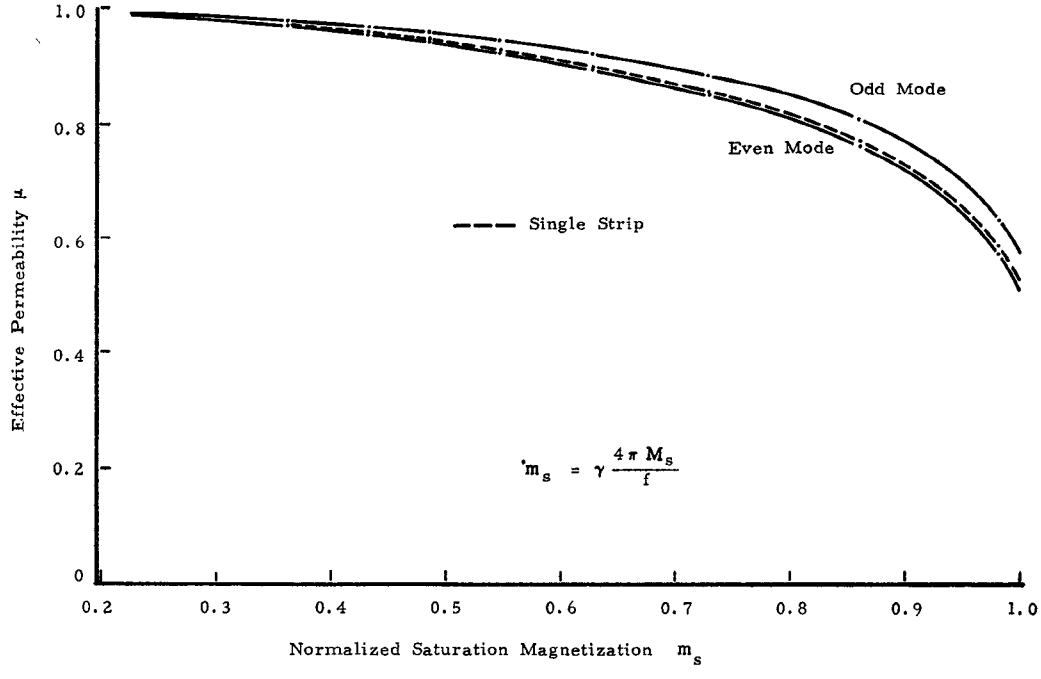

Fig. 2. Effective permeability versus normalized saturation magnetization for coupled microstrip lines on a demagnetized ferrite substrate: $K = 14.4$.

By superposition, the terminal voltages for the coupled strips become

$$\begin{aligned} V_1 &= (v_{a1} + v_{a2} + v_{a3} + v_{a4})\big|_{x=0} \\ V_2 &= (v_{b1} + v_{b2} + v_{b3} + v_{b4})\big|_{x=0} \\ V_3 &= (v_{b1} + v_{b2} + v_{b3} + v_{b4})\big|_{x=l} \\ V_4 &= (v_{a1} + v_{a2} + v_{a3} + v_{a4})\big|_{x=l}. \end{aligned} \tag{4}$$

For the case of a single meander line, the configuration of Fig. 1 must be changed to include a short strap connecting terminal 3 with terminal 4, thus completing the circuit. This requires the constraint that $I_3 = -I_4$ and $V_4 = V_3$.

Substitution of (2), (3), and similar expressions into (4), applying the meander-line constraint at terminals 3 and 4, and simplifying with (1), the terminal voltages are given in two-terminal open-circuit impedance form as

$$\begin{aligned} V_1 &= z_{11}I_1 + z_{12}I_2 \\ V_2 &= z_{21}I_1 + z_{22}I_2 \end{aligned}$$

with

$$z_{11} = z_{22} = \left[\frac{-j}{2}\frac{Z_{0e}\cos\beta_e l}{\sin\beta_e l} - \frac{j}{2}\frac{Z_{0o}\cos\beta_o l}{\sin\beta_o l} + \frac{j}{2}\frac{Z_{0o}}{\sin\beta_o l\cos\beta_o l}\right]$$

and

$$z_{12} = z_{21} = \left[\frac{-j}{2}\frac{Z_{0e}\cos\beta_e l}{\sin\beta_e l} + \frac{j}{2}\frac{Z_{0o}\cos\beta_o l}{\sin\beta_o l} - \frac{j}{2}\frac{Z_{0o}}{\sin\beta_o l\cos\beta_o l}\right]. \tag{5}$$

The image impedance [2] of such a symmetrical two-terminal pair network is

$$Z_I = \sqrt{\frac{z_{11}}{z_{22}}|z|} = \sqrt{z_{11}z_{22} - z_{12}z_{21}} \tag{6}$$

with the determinant $|z| = z_{11}z_{22} - z_{12}z_{21}$. Substitution of the component parts of (5) into (6) gives the image impedance of the basic meander line as

$$Z_I = \sqrt{Z_{0e}Z_{0o}}\sqrt{\frac{\tan\beta_o l}{\tan\beta_e l}} \tag{7}$$

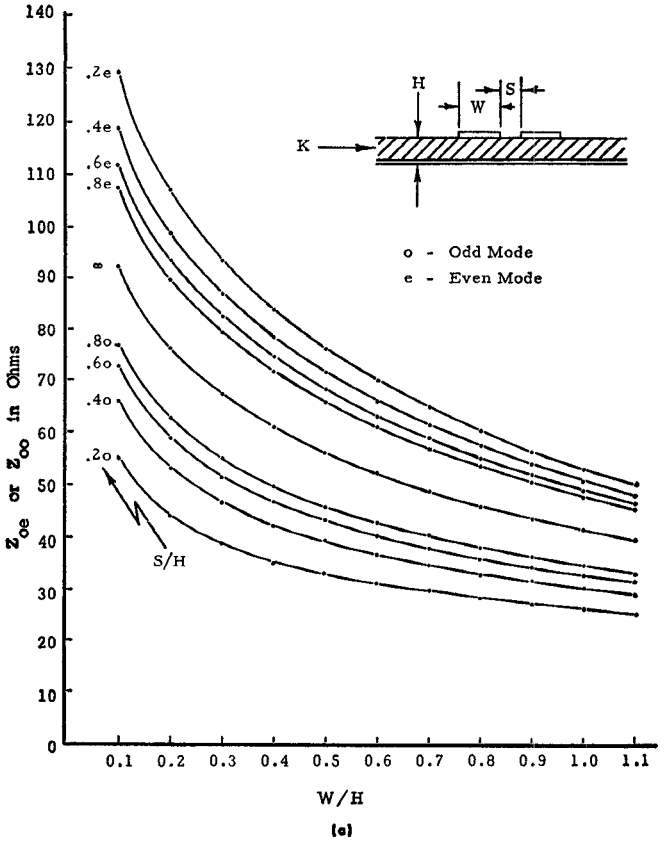

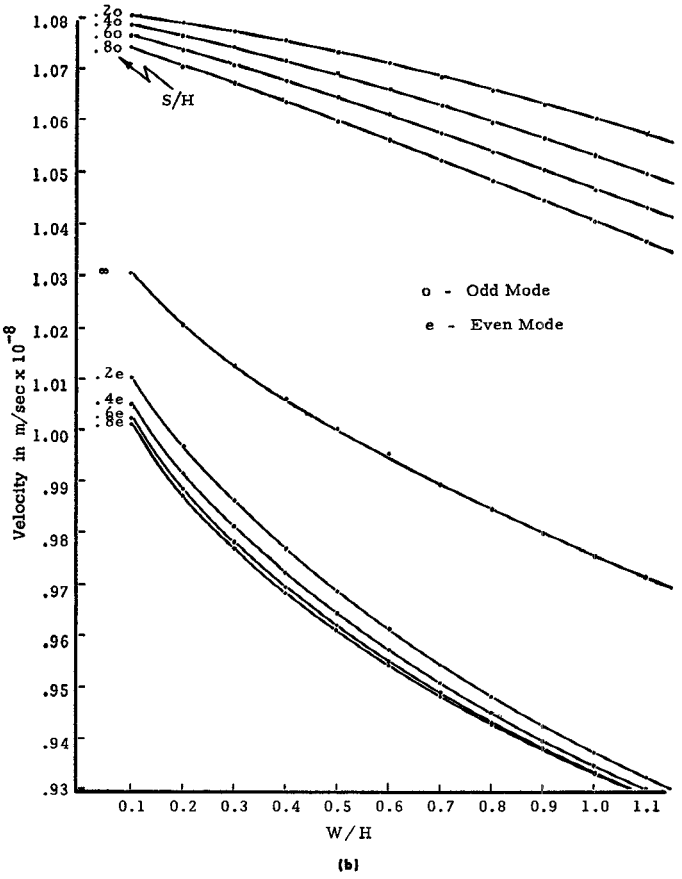

Fig. 3. (a) Even- and odd-mode impedances for coupled microstrips with parameter S/H: substrate $K=14.4$ (dielectric). (b) Even- and odd-mode velocities for coupled microstrips with parameter S/H: substrate $K=14.4$ (dielectric).

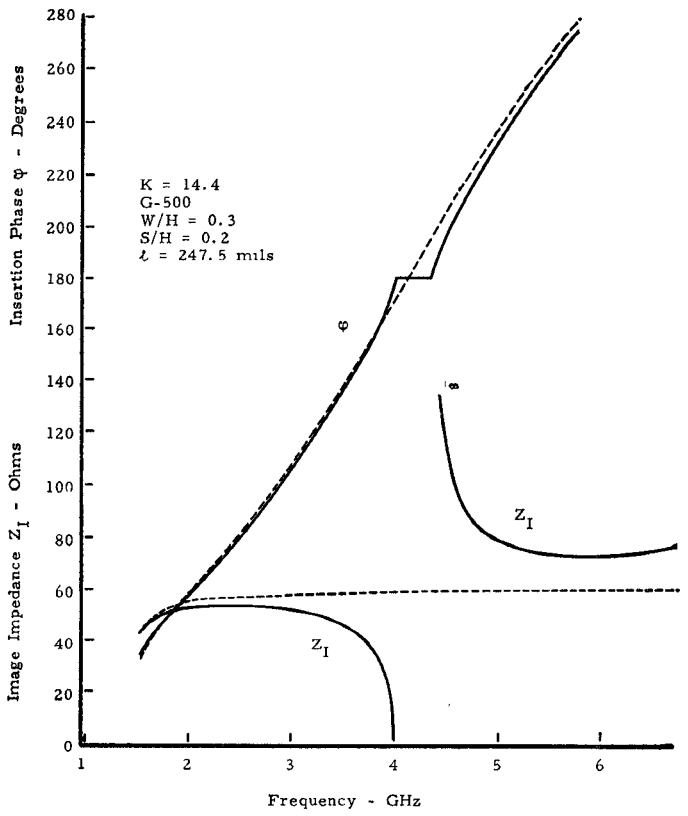

Fig. 4. Theoretical image impedance and insertion phase of a microstrip meander line on a demagnetized ferrite (G500) substrate.

where the second radical results from preserving the separate identities of even- and odd-mode velocities.

The image transfer constant [2] for any two-port network is defined in impedance terms as

$$\cosh\theta = \frac{(z_{11}z_{22})^{1/2}}{z_{12}} \tag{8}$$

where $\theta=\alpha+j\phi$. Substituting from (5), and using the assumed lossless condition, (8) becomes

$$\cos\phi = \frac{Z_{0e}/Z_{0o} - \tan\beta_e l \tan\beta_o l}{Z_{0e}/Z_{0o} + \tan\beta_e l \tan\beta_o l}. \tag{9}$$

An examination of the Weiss–Bryant [3] data reveals that $\beta_o<\beta_e$ for coupled microstrips. Thus coupling in microstrip makes the basic meander line a bandpass filter, for when $\beta_o l<\pi/2<\beta_e l$ the image impedance of (7) is imaginary and therefore the filter is in cutoff. Presence of a stopband in the expected performance merely indicates a frequency range where operation must be avoided; it has little bearing on the intended application.

Design Details

Interest in small amounts of switchable nonreciprocal phase shift prompts the design of a line having only two meanders with an image impedance of approximately 50 Ω at 3 GHz. It is assumed that the coupling of the two meanders produces a negligible effect on Z_I.

The ferrite substrate selected is G500 having a magnetic saturation moment $4\pi M_s=550$ G and a dielectric constant of 14.4. The effect of frequency on the permeability μ in the demagnetized state for G500 ferrite is illustrated in Fig. 2.[1] Although the substrate magnetization normally is latched in one of its remanent states, little error exists if the scalar demagnetized μ is used for calculations.[2]

[1] The data are reproduced with permission from E. J. Denlinger of the Lincoln Laboratory staff.

[2] Using Denlinger's results [4] based on Schlömann's curves [5] and latched magnetization, the effective permeability (average of forward- and reverse-propagation directions) may be calculated for each mode. Providing $m_s<0.8$, these calculations are very close to values of the demagnetized μ.

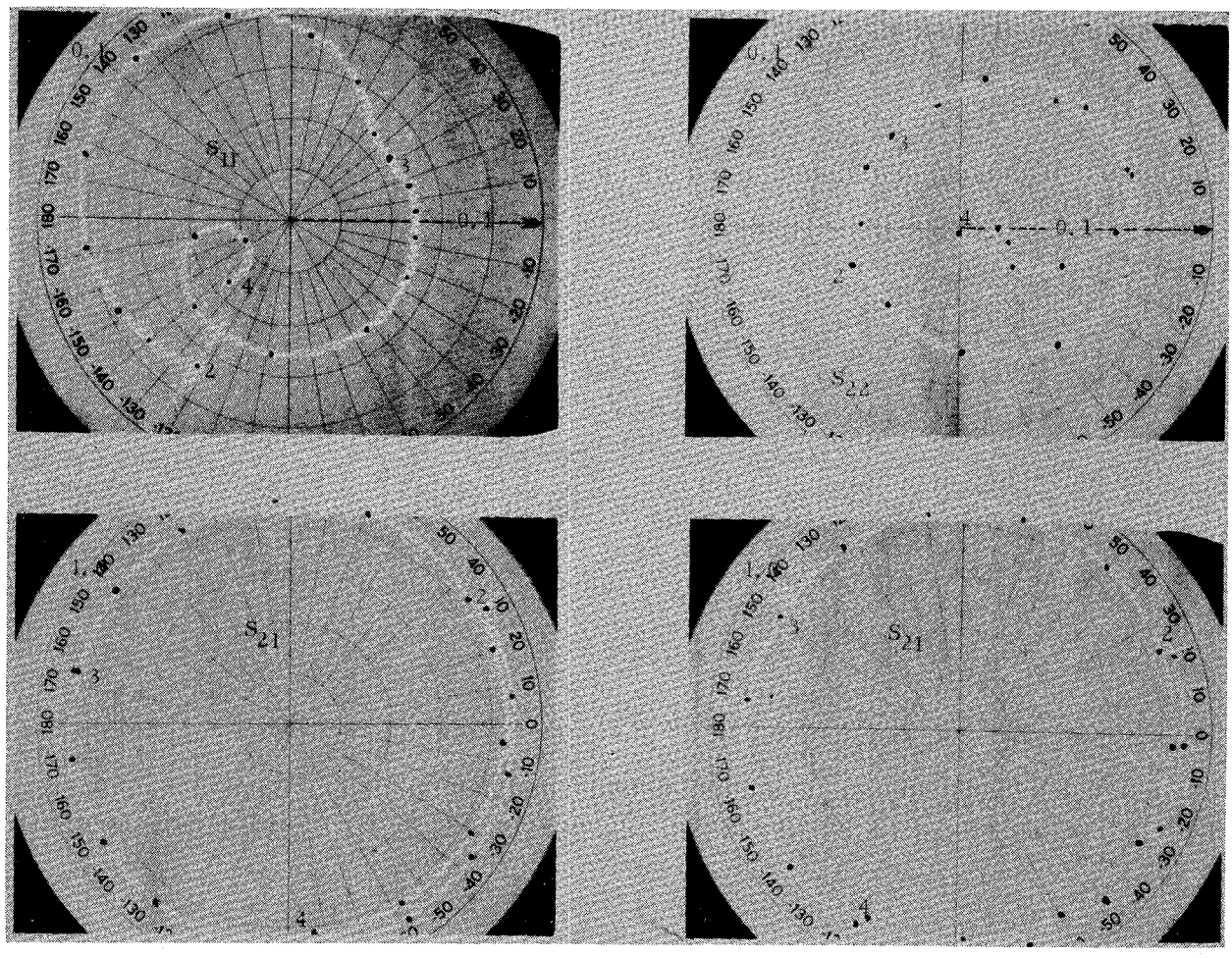

Fig. 5. Scattering parameters for an experimental two-meander chrome–gold line on G500 ferrite: Graphs are swept from 2 to 4 GHz.

Choice of stripwidth W for a straight feed line must be made taking into account the fact that Z_I is a function of μ. For example Z_I (dielectric) $= (50/\sqrt{0.933}) = 51.76\ \Omega$ at 3 GHz. Fig. 3(a) and (b) show the Weiss–Bryant[3] data calculated for a dielectric ($K = 14.4$) substrate. From these curves $W/H = 0.602$ for 51.76 Ω or on a 40-mil substrate $W = 24$ mil.

For the meander line choices must be made of spacing (S/H) as well as strip width (W/H). In this case both the even- and odd-mode impedances together with the even- and odd-mode propagation constants β_e and β_o are proportional to the square root of their respective permeabilities. Tight coupling is selected for this case with $S/H = 0.2$. Selecting $W/H = 0.3$ for the meander legs gives $Z_I = 52.3\ \Omega$ at 3 GHz. The length of the meander legs is selected as 247.5 mil to give $\beta_e l = \pi/2$ at S-band limit of 4 GHz.

Fig. 4 shows both the image impedance Z_I and the insertion phase ϕ calculated with (7) and (9) for this designed line at frequencies in L, S, and C bands. The dashed curves are intended to show the character of Z_I and of ϕ if the effect of different even- and odd-mode velocities is not taken into account.

Measured Results

An experimental model with two meanders was formed by depositing chrome–gold to a thickness of 0.354 mil on a G500 substrate. Caulton *et al.* [6], develop an approximate width correction which for this thickness amounts to 0.7 mil.

Owing to printing and etching inaccuracies, the deposited meander-line dimensions were different from the design. The width of the average meander leg was 10.13 mil instead of the expected 12 mil, while the average spacing was increased to 9.36 mil compared to the design of 8 mil. The straight feed linewidth was 20.67 mil.

[3] These data were kindly furnished by J. A. Weiss and T. G. Bryant with use of their computer program [3].

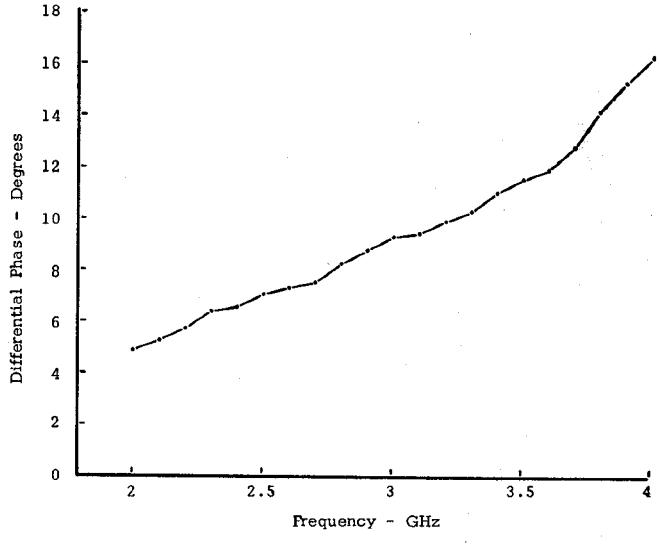

Fig. 6. Differential phase shift versus frequency for a two-meander chrome–gold line on G500 ferrite.

Recalculation of the image impedances using these dimensions with the Caulton width correction yields $Z_I = 52.3\ \Omega$ for the feed line and $Z_I = 54.93\ \Omega$ for the meander line itself.

A set of measured scattering parameters for this experimental line is shown in Fig. 5. Frequency intervals of 0.1 GHz are marked with dots along the entire 2–4 GHz range of the graphs. The scale for both S_{11} and S_{22} has been expanded to 0.1 full scale. Transmission

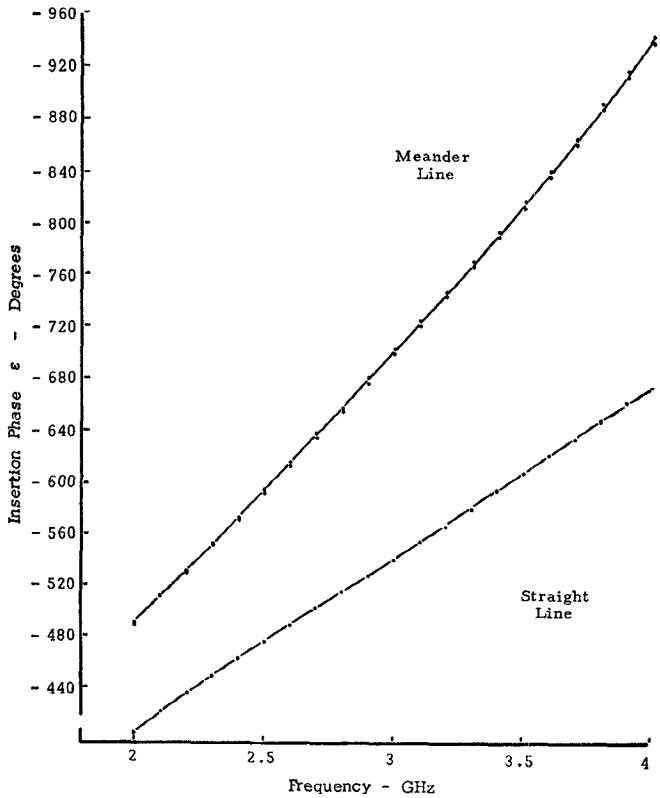

Fig. 7. Insertion phase versus frequency for a line with two meanders and a straight line both on a 2-in ferrite G500 substrate.

coefficient S_{21} is shown for the two latched directions of magnetization. Although S_{12} measurements are not shown, they were within experimental error of 1° from S_{21} values with the latching reversed. At higher frequencies the meander line shows the beginning of cutoff, for S_{11} was measured as 0.5 at 5.25 GHz. S_{11} becomes 0.7 at 5.6 GHz. There is evidence indicating that coupling one basic meander to another causes a shift in the predicted cutoff frequency.

There is no known direct way to calculate nonreciprocal differential phase shift. Thus Fig. 6 shows the measured phase shift of this experimental line at frequencies in S band. Measurements on a straight line deposited on the same substrate allow the insertion phase of the meander line alone to be determined.
These measurements are shown in Fig. 7.

Conclusions

The experimental results clearly verify that a desired image impedance of a line with few meanders can be achieved using the outlined procedure. Tolerance in dimensions shows that tradeoff is possible between strip spacing and leg width for the same meander line Z_I. The theoretical bandpass characteristic predicted is supported by the tendency for the line to show cutoff at 5.25 GHz. With only two tightly coupled meanders operating near 3 GHz, the data show 10° of switchable nonreciprocal differential phase shift to be possible. The precise effect on cutoff frequency and impedance of coupling one basic meander to another together with the demonstration of a way to calculate meander-line nonreciprocal differential phase shift remain subjects for further research.

Acknowledgment

The author wishes to thank C. Blake of Lincoln Laboratory for making the research possible, and Dr. J. A. Weiss, Consultant to Lincoln Laboratory, for his valuable advice and criticism.

References

[1] E. M. T. Jones and J. T. Bolljahn, "Coupled-strip-transmission-line filters and directional couplers," *IRE Trans. Microwave Theory Tech.*, vol. MTT-4, pp. 75—81, Apr. 1956.
[2] E. A. Guillemin, *Communication Networks*, vol. II. New York: Wiley, 1935, pp. 173—175.
[3] T. G. Bryant and J. A. Weiss, "Parameters of microstrip transmission lines and of coupled pairs of microstrip lines," *IEEE Trans. Microwave Theory Tech. (1968 Symposium Issue)*, vol. MTT-16, pp. 1021–1027, Dec. 1968.
[4] E. J. Denlinger, "Dynamic solutions for single and coupled microstrip lines," M.I.T. Lincoln Lab., Lexington, Mass., Tech. Rep. 470, Nov. 1969.
[5] E. Schlömann, "Microwave behavior of partially magnetized ferrites," *J. Appl. Phys.*, vol. 41, pp. 204–214, Jan. 1970.
[6] M. Caulton, J. J. Hughes, and H. Sobol, "Measurements on the properties of microstrip transmission lines for microwave integrated circuits," *RCA Rev.*, vol. 3, pp. 377–391, Sept. 1966.

Mode Chart for Microstrip Ring Resonators

Y. S. WU AND F. J. ROSENBAUM

***Abstract*—A universal mode chart for the microstrip ring resonator, based on a radial waveguide model, is presented. The resonant frequency is related to the width of the ring conductor. Experimental results from 4 to 16 GHz are shown to be in good agreement with the theory.**

Introduction

Ring resonators have found application in circulators, hybrid junctions, filters, and other microstrip devices. Troughton [1] and Caulton *et al* [2]. have used them to measure propagation constants in microstrip, based on the principle that the ring is resonant when its mean circumference equals an integral number of wavelengths. Wolff and Knoppik [3] have recently shown that there are dispersive effects that must be considered, as well as the influence of the ring center conductor width on the resonant frequency. This short paper presents a universal mode chart for ring resonators, relating the resonant frequency to the ring width and its mean circumference. Qualitative agreement is shown with experimental results. Quantitative agreement may be obtained by modifying the effective dielectric constant of the substrate according to Wheeler's approximation [4].

Theory

Fig. 1 shows the geometry of the resonator whose mean radius is $R=(a+b)/2$. If the electromagnetic fields are assumed to be confined to the dielectric volume between the perfectly conducting ground plane and the ring conductor, then the fields may be shown to be TM to z [3]. The field components are E_z, H_r, and H_ϕ and the resonant modes are denoted as TM_{nml}. For the thin substrates normally encountered in microwave integrated circuits, the fields may be taken as independent of the z coordinate ($l=0$).

The fields propagate in the radial direction and may have ϕ variation. Application of the usual magnetic wall boundary conditions at $r=a$; $r=b$, typically assumed for wide microstrip [5], [6] leads to the well-known characteristic equation for the resonant modes:

$$J_n'(ka)\,Y_n'(kb) - J_n'(kb)\,Y_n'(ka) = 0 \tag{1}$$

with

$$k = \frac{\omega}{c}\sqrt{\epsilon_d} \tag{2}$$

where ω is the resonant radian frequency, c is the speed of light in vacuo, and ϵ_d is the relative dielectric constant of the substrate. The quantities $J_n(x)$ and $Y_n(x)$ are Bessel's functions of the first and second kind, order n, respectively, and the prime denotes derivatives with respect to kr. The integer n is the azimuthal mode number. Notice that (1) is the same equation satisfied by TE modes in coaxial waveguides [7]. The use of idealized boundary conditions is discussed later.

For narrow microstrip widths ($a \simeq b$), (1) reduces to

$$[(ka)^2 - n^2][J_{n-1}(ka)\,Y_n(ka) - Y_{n-1}(ka)J_n(ka)] = 0. \tag{3}$$

Manuscript received May 12, 1972; revised February 26, 1973. This work was sponsored by the United States Air Force Avionics Laboratory, WPAFB, Dayton, Ohio, under Contract F33615-72-C-1054.

Y. S. Wu was with the Department of Electrical Engineering, Washington University, St. Louis Mo. 63130. He is now with the School of Electrical Engineering, Cornell University, Ithaca, N.Y. 14850.
F. J. Rosenbaum is with the Department of Electrical Engineering, Washington University, St. Louis, Mo. 63130.